(307) No: E49/[redacted]

MSC INTERNAL NOTE NO. 65-EG-49

PROJECT APOLLO

ANALYSIS OF LUNAR LANDING SIMULATION RESULTS AS APPLIED TO LANDING DESIGN CRITERIA

Prepared by: Richard Reid

Richard Reid
Engineering Simulation Branch, GCD

and

Alan H. Feiveson

Alan H. Feiveson
Theory & Analysis Office, Comp. & Anal.

Approved: Charles J. Mackin
for David W. Gilbert, Chief,
Engineering Simulation Branch, GCD

Approved: R. G. Chilton
Robert G. Chilton, Deputy Chief,
Guidance and Control Division

Approved: Eugene L. Davis
Eugene L. Davis, Jr., Chief
Theory & Analysis Office, Comp. & Anal.

Approved: Eugene H. Brock
Eugene H. Brock, Chief,
Computation and Analysis Division

NATIONAL AERONAUTICS AND SPACE ADMINISTRATION

MANNED SPACECRAFT CENTER

Houston, Texas

November 12, 1965

SUMMARY

A statistical analysis of data from a piloted simulation study of the lunar landing maneuver has been made. The purpose of this analysis was to determine probability of the piloted landing being within the present landing gear design envelope. Consideration was given to all possible error sources influencing touchdown control. The significant error sources were statistically added to the simulation data, and the combined data used to determine probability contours and numbers.

The results of this analysis indicated the velocities at touchdown for a manually controlled landing have a probability of 0.9976 of being within the present design envelope even with what is considered a pessimistic error model. The angular rates have high probability of being within design when considered individually. It was not possible to compute a combined probability for the three rates being within the design limit, but the range of the individual rates for 0.99 probability was sufficiently small to indicate a combined probability number would be quite high. However, the present angular design limit appears to be too small for the expected angular excursions at touchdown. The analysis indicated the probability of being within the angular limits was 0.9678. The probability number could be increased by changing the design limits or repositioning the center of gravity offset existing in the LEM at touchdown. The latter change would eliminate the bias in spacecraft attitude which is the primary cause of the low probability of being within the angular limits.

INTRODUCTION

The results of previous piloted simulation studies of the lunar landing maneuver have generally been presented in the form of the upper and lower boundaries of touchdown conditions. Results presented in this form provide a quantitative measure of the pilot's ability to safely control the landing maneuver. However, analyses of this type fail to adequately define the true situation as to the probability of the pilot being able to control the spacecraft to within the present landing gear design limits. Because of this, the Guidance and Control Division and the Computation and Analysis Division have analyzed the results of a previous simulation study of the lunar landing maneuver (reference 1) to obtain the statistical properties of the pilot controlled landing data. The effect of accelerometer bias, inertial measurement unit (IMU) gimbal angle misalinement, and radar errors on the touchdown criteria are included by statistically adding the expected errors resulting from these sources to the pilot controlled data of reference 1.

DATA SOURCES

The data used in this analysis was obtained from the results of the simulation study discussed in reference 1. These data consist of velocity and angular conditions existing at touchdown and were obtained from 300 landings made by five separate pilots. In addition, the data of reference 1 were also extended by back calculating the known touchdown conditions to obtain velocity and angular conditions at probe contact, then recalculating touchdown conditions for a different probe length and engine delay time. The techniques and the necessary assumptions used to perform these calculations are explained in appendix A.

ERROR SOURCES

The primary sources of errors affecting landing touchdown control are (1) the pilot-display combination, (2) the guidance and control system and its sensors, and (3) the physical characteristics of the spacecraft. An analysis of these three areas indicated that the following specific items were the major contributing error sources:

Control System Response
Landing Radar Velocity Measurement
Landing Radar Altitude Measurement
IMU Accelerometer Bias
IMU Gimbal Misalinement
Display System
Pilot
C. G. Position

Examination of these error sources shows that at least two--control system response and radar altitude measurement--have little effect on touchdown control. The effect of control system response errors is small because of the relatively short control system response time. Landing radar altitude measurement errors do not contribute to the errors because a probe was used to sense the altitude at which the descent engine was shut down.

The system error sources considered, then, were: (1) landing radar velocity measurement, (2) IMU accelerometer bias, (3) IMU gimbal angle misalinement, (4) pilot-velocity display errors, and (5) C. G. position. It was necessary to combine the errors caused by pilot control and velocity display errors and resolution because they comprise a single system insofar as measurement of these errors is concerned. The IMU accelerometer bias error was assumed to be 0.0165 ft/sec^2, the IMU gimbal angle misalinement used in the study was 0.05 degree (1σ). Radar velocity errors considered represented the upper and lower bounds for the present landing radar. The c. g. location data used in this analysis was obtained from the mass properties data of the LEM spacecraft. A listing of these errors and the statistical combinations for all of the sources considered is given in table 1.

SCOPE OF ANALYSIS

Probability contours and probability numbers for being within the present design criteria were determined using the reference 1 and modified reference 1 data in combination with the error sources noted in the previous section. The contours for velocity and angular position were obtained for landings with manual and automatic engine shutoff. The error source combinations and their magnitudes are given in table 1.

STATISTICAL ANALYSIS TECHNIQUES

The technique used to combine the basic and modified reference 1 data and the error models consisted of using a random process adding of the error models to the data on a per run basis. This was necessary because the velocity data for the 300 runs of reference 1 without radar or IMU errors failed to test normal using the Kolmogorov-Smirnov normalcy test. The horizontal velocity vector was obtained by taking the root-sum-square (RSS) of the forward and lateral velocities after the random process adding of the error models had been completed. The techniques for determining the various probability contours and the probability of being within the landing gear design criteria are given in appendices A and B.

DISCUSSION OF RESULTS

The results of this analysis are presented in three sections: (1) a discussion of the velocity probability contours and their application to the design envelope, the effect of varying simulation conditions, and the effect of the different error sources on the probability contours, (2) a discussion of the probability contours for the roll and pitch angles at touchdown along with a discussion of the effect of c.g. uncertainties on touchdown angles, and (3) a discussion of the expected range of angular rates at touchdown.

Effect of Error Sources on Touchdown Velocities

The velocity probability contours were calculated as discussed in appendix B. These contours were then plotted as a function of horizontal and vertical velocity and compared to the present landing gear velocity design limits (indicated in the figures as a dashed line) of 10-7-4. In addition, the probability of being within the velocity profile has been calculated and the results listed in table 2 for the various combinations of data and error sources.

Reference 1 Data Plus Pessimistic Radar Errors - The probability contours for the reference 1 data plus pessimistic radar errors indicates the 0.99 contour to be completely within the design envelope (figure 1). The 0.999 contour lies slightly outside the design profile between 4 and 7 feet/second, but table 2 shows the probability of being within the design envelope is 0.9944. The error model in this case, however, reflects a pessimistic radar performance, and thus, the probability of being within the 10-7-4 envelope increases as smaller radar errors are assumed.

Modified Data Pessimistic Radar and IMU Errors - The contours calculated for the modified data plus the pessimistic radar and IMU errors shown in figure 2 reveal that the contours have expanded slightly because of the increased velocities caused by the addition of IMU gimbal angle misalinement and uncompensated accelerometer bias errors. Because the effect of the increased probe length is more than compensated for by the longer engine delay time and decreased descent velocity, the contours have shifted slightly downward along the vertical axis. Even though the contours are slightly expanded compared to those of figure 1, the probability of being within the 10-7-4 design envelope has increased to 0.9976. The higher probability number reflects the effect of the general downward shift of the contours.

Effect of Error Sources on Touchdown Velocity - To determine the effect of the various error sources on the probability contours, the 0.99 contours for the modified reference 1 data plus the pessimistic radar errors and IMU errors and the modified reference 1 data plus optimistic radar errors and IMU errors were determined. In addition, the 0.99 contours for the error sources without the pilot data were also determined. The results of the calculations are shown by the contours of figures 3 and 4. Figure 3 shows the 0.99 for the pilot plus the pessimistic radar and IMU errors just

touches the 4 ft/sec design limit whereas figure 4 shows the 0.99 contour for the system errors alone has a maximum boundary limit of about 3.5 ft/sec. This shows that for the pessimistic radar errors, the errors are the major factor in setting the contour boundaries. When the optimistic radar error contours of figures 3 and 4 are compared, it is seen that system errors and pilot errors have an approximately equal contribution to setting the contour boundary. The contours of figure 4 also very nearly approximate automatic landing performance with the same errors present. (Reference 2)

Effect of Automatic Engine Shutoff on Touchdown Velocity Control - The effect of an automatic descent engine shutdown on the control velocity is shown in figure 5. These curves were calculated assuming a 1.5 foot probe length using the modified reference 1 data. A comparison of this figure and the 0.99 probability contour of figure 2 shows that an automatic descent engine shutoff affects only the vertical shape of the contour. The automatic engine shutoff causes the mean vertical touchdown velocity to be of the order of 1 ft/sec lower than the manual engine shutoff for the conditions assumed (1.5 ft. probe, .25 sec engine delay). The vertical spread of the contour, however, is slightly greater in the automatic case because for the manual engine shutdown, the variable pilot reaction time to the probe contact indication causes a compression of the contour.

Probability of Being Within Angular Limits at Touchdown

The 0.9, 0.99, and 0.999 contours for the pitch and roll angles for the simulation data of reference 1 are shown in figure 6. The figure shows that even a small portion of the 0.9 contour lies outside the present design limit (dashed line). This can be attributed directly to the one-inch lateral c.g. offset used in the study of reference 1. Had the c.g. offset (which is present in the actual LEM) been zero, the probability contours would have been symmetrical about the origin, and it is possible in this case that most of the 0.99 contour would be inside the design envelope. The probability of being within the design envelope in the presence of a constant one-inch lateral c.g. offset is 0.9678 (table 2).

Effect of C.G. Uncertainties on Touchdown Angles - Figure 7 shows the 0.99 probability contours for a one-inch c.g. offset and a 0.90 probability of one inch or less c.g. uncertainty. The effect of the additional one-inch uncertainty is to force more of the contour outside the design envelope. Contrary to the preceding case, removal of the one-inch bias would not result in most of the 0.99 contour being within the design limits. The probability of being within the design with the additional one-inch uncertainty is given in table 2 as 0.8806.

Probability of Being Within Angular Rate Limit at Touchdown

The angular rates from reference 1 data tested both dependent and non-normal which prevents determining the probability contours. However, the probability number for being within the design limit can be calculated using order statistics, the details of which are given in reference 3. The 0.99 probability computation shows that the confidence of the rates being within this limit is only 0.35 for pitch and 0.58 for roll and yaw. However, all rates are well inside the design limit with the maximum value of angular rate being roll rate which is 2.22 deg/sec. Thus, while the confidence associated with the 0.99 number is low, it is unlikely that any angular rate will exceed the present 3 deg/sec design limit.

CONCLUDING REMARKS

The statistical analysis presented in this report indicates the touchdown velocities are primarily influenced by the magnitudes of the system errors assumed. The contours shown in the results can be adjusted to some degree by varying engine delay time, probe length, and the descent velocity profile. As the actual system errors become better defined, the techniques used in this report can be used to analyze and determine their impact on landing criteria. The angle results of this study show a definite need for making the c.g. bias and uncertainties as small as possible at touchdown. For conditions as they are now known, the angular limits of the design criteria appears to be too small for the expected attitudes of a normal landing maneuver.

REFERENCES

1. Project Apollo Internal Note No. 65-EG-35 entitled "A Preliminary Simulation Study of the Required Velocity Meter Sensitivity and Touchdown Control Performance During Lunar Landing," by Richard Reid and Herbert G. Patterson.

2. Project Apollo Internal Note No. 65-EG-36 entitled "A Study of Automatically Controlled LEM Landings", by W. H. Peters and D. A. Dyer.

3. An Introduction to Mathematical Statistics, H. D. Brunk, Ginn and Co., 1960.

ERROR MODEL	Velocity Component	Uncompensated Accelerometer Bias (ft/sec^2)	IMU Gimbal Angle Misalinement (deg)	Landing Radar (ft/sec)	Total (ft/sec)
2 I	Vertical	0	0	0.50	0.50 [1]
	Forward	0	0	1.00	1.00
	Lateral	0	0	0.90	0.90
2 II	Vertical	0.0165	0	0.50	.501 [1]
	Forward	0.0165	0.05	1.00	1.02
	Lateral	0.0165	0.05	0.90	0.922
3 III	Vertical	.0043	0	0.260	0.262
	Forward	.0043	.042	0.270	0.340
	Lateral	.0043	.042	0.500	0.522

Note: All values given are standard deviation about zero mean

1. Accelerometer bias and gimbal angle misalinement converted to equivalent velocity error assuming a 20-second descent after final computer update

2. Pessimistic radar errors

3. Optimistic radar errors

Table 1 - Error Models Used for Statistical Analysis

Translation Velocities

Pr $\{10, 7\text{-}4\}$; Basic Data Plus Error Model 1 = 0.9962

Pr $\{10, 7\text{-}4\}$; Modified Data Plus Error Model 2 = 0.9976

Angles

Pr $\{3, 3\}$; No c.g. variations = 0.9678

Pr $\{3, 3\}$; 1" 1 σ c.g. variation = 0.8806

Angular Rate

Pr $\{-1.59 < p < 2.22\}$ = 0.99 , .58 conf.

Pr $\{-2.08 < q < 1.59\}$ = 0.99 , .35 conf.

Pr $\{-.18 < r < .45\}$ = 0.99 , .58 conf.

TABLE 2 - PROBABILITIES OF BEING WITHIN SPECIFIED LIMITS

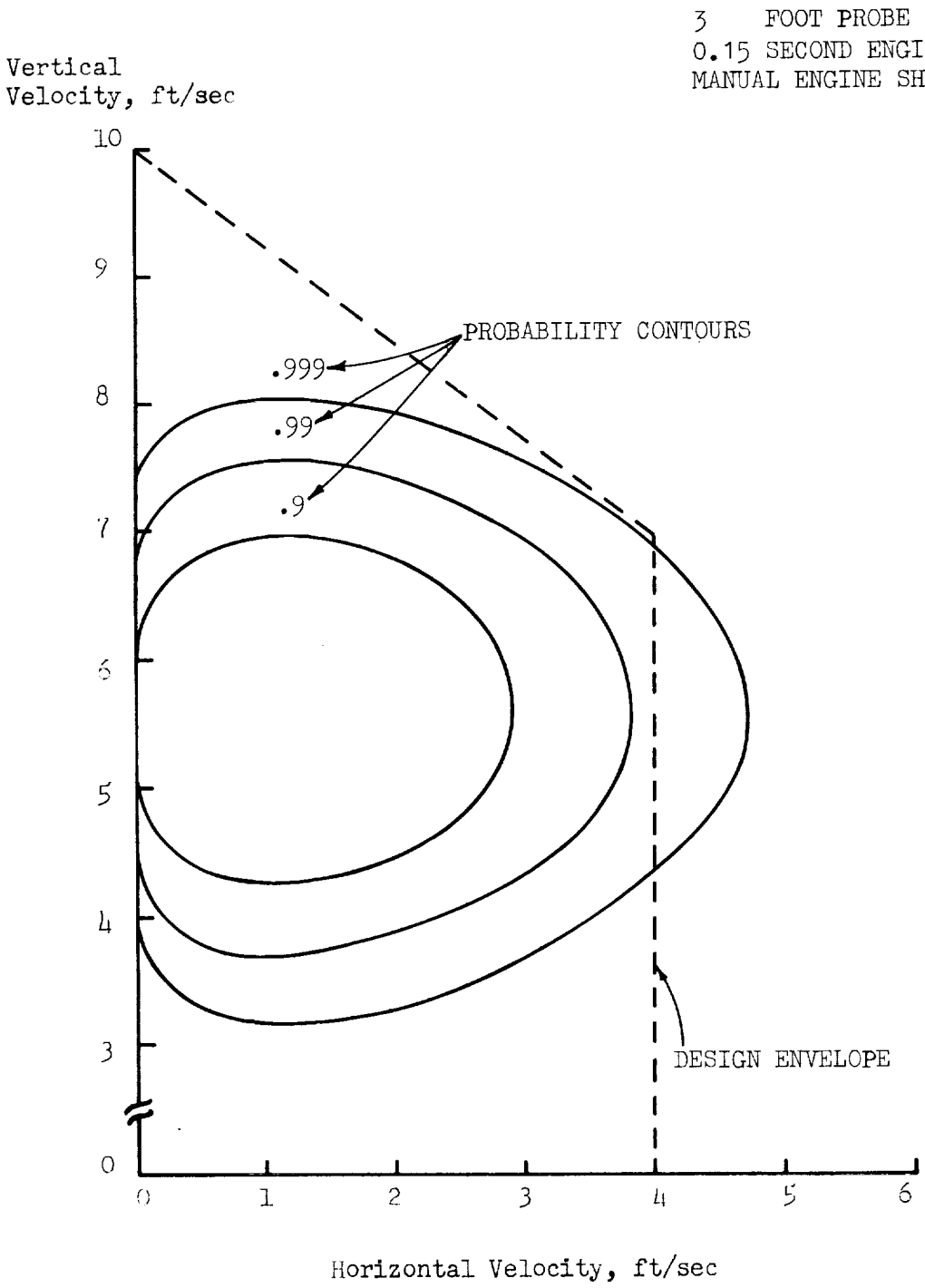

FIGURE 1. PROBABILITY CONTOURS FOR TOUCHDOWN VELOCITY.
(REFERENCE 1 DATA PLUS PESSIMISTIC RADAR ERRORS)

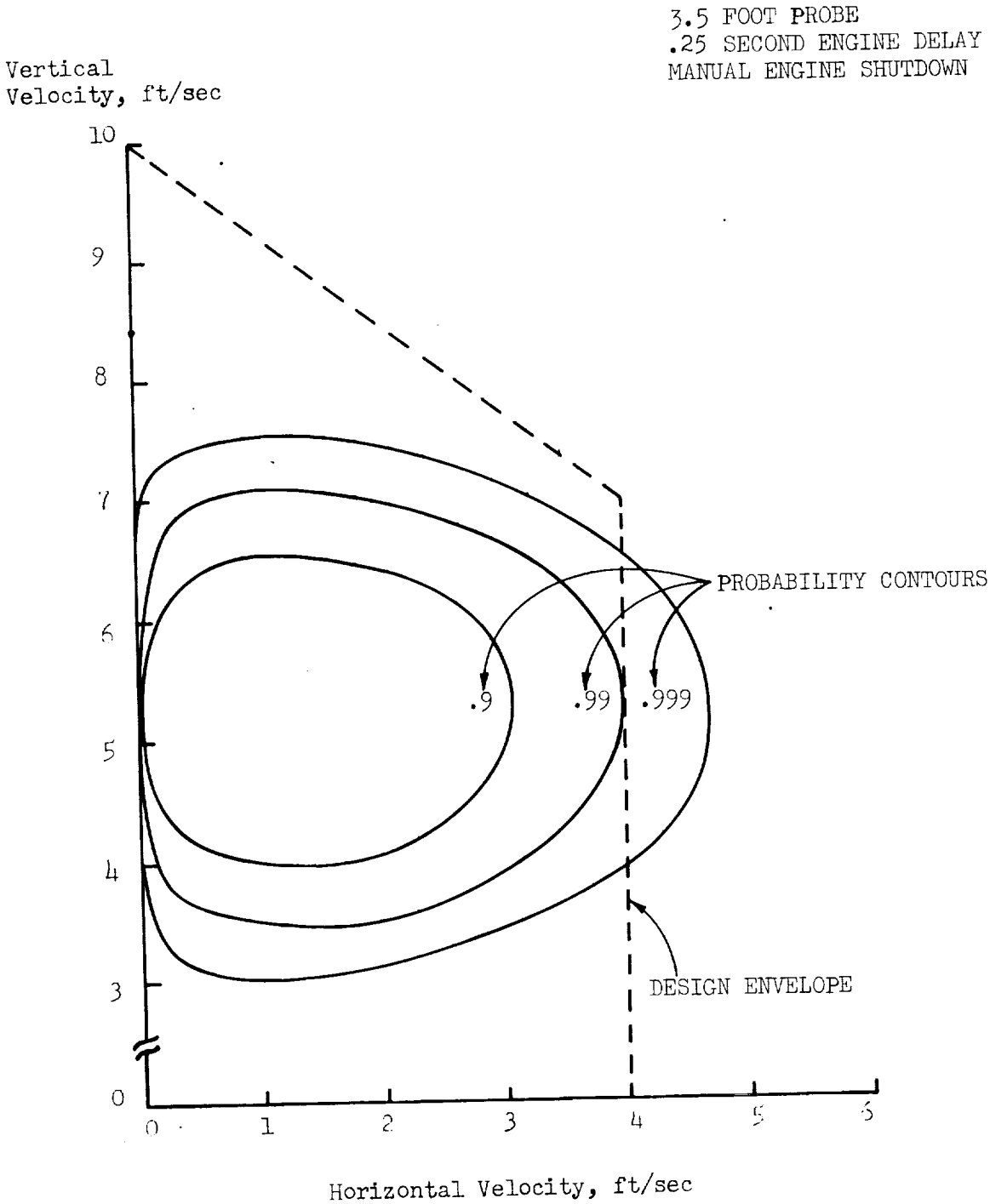

FIGURE 2. PROBABILITY CONTOURS FOR TOUCHDOWN VELOCITY.
(MODIFIED REFERENCE 1 DATA PLUS PESSIMISTIC RADAR ERRORS AND IMU ERRORS)

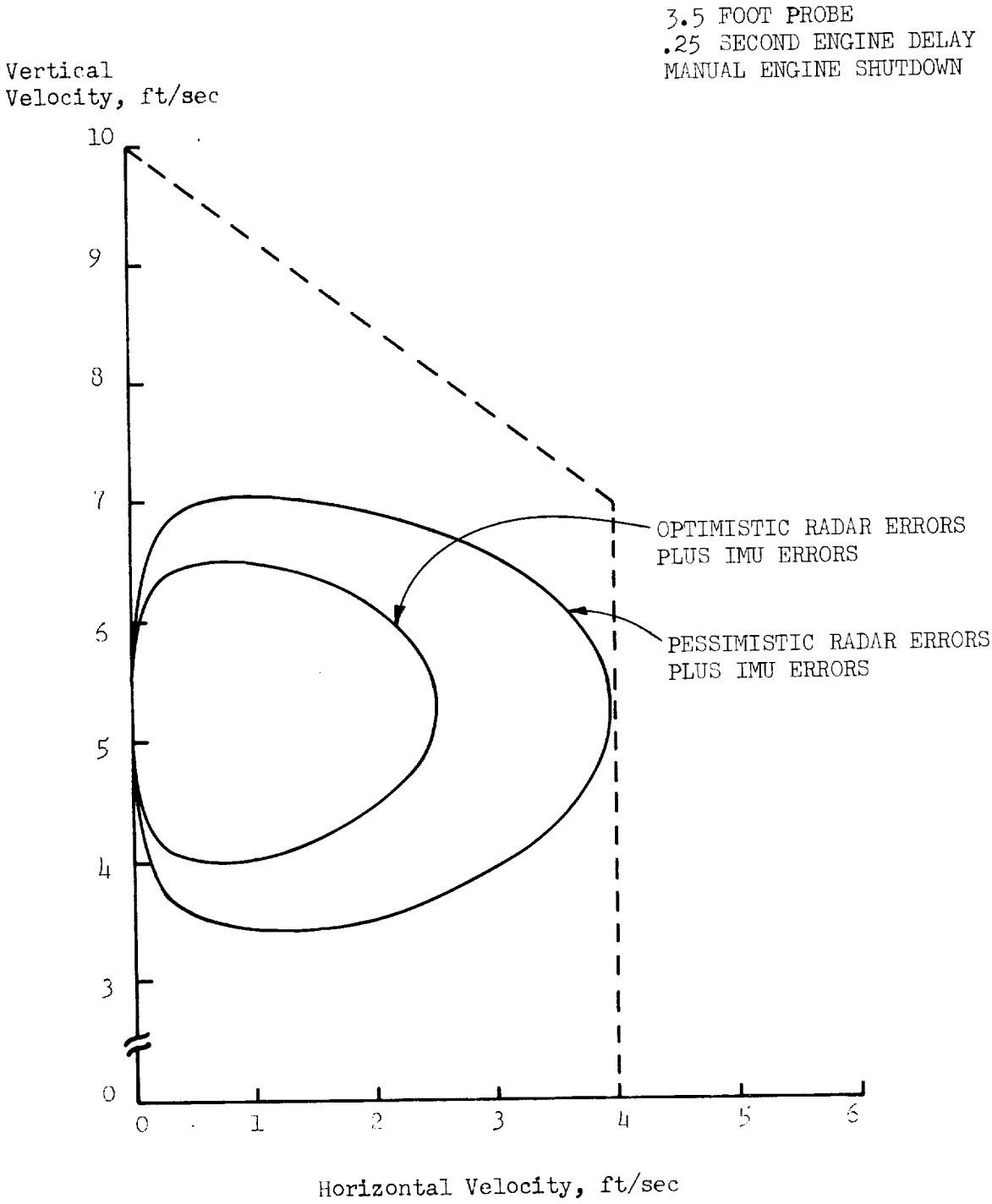

FIGURE 3. 0.99 PROBABILITY CONTOURS FOR TOUCHDOWN VELOCITY.
(MODIFIED REFERENCE 1 DATA)

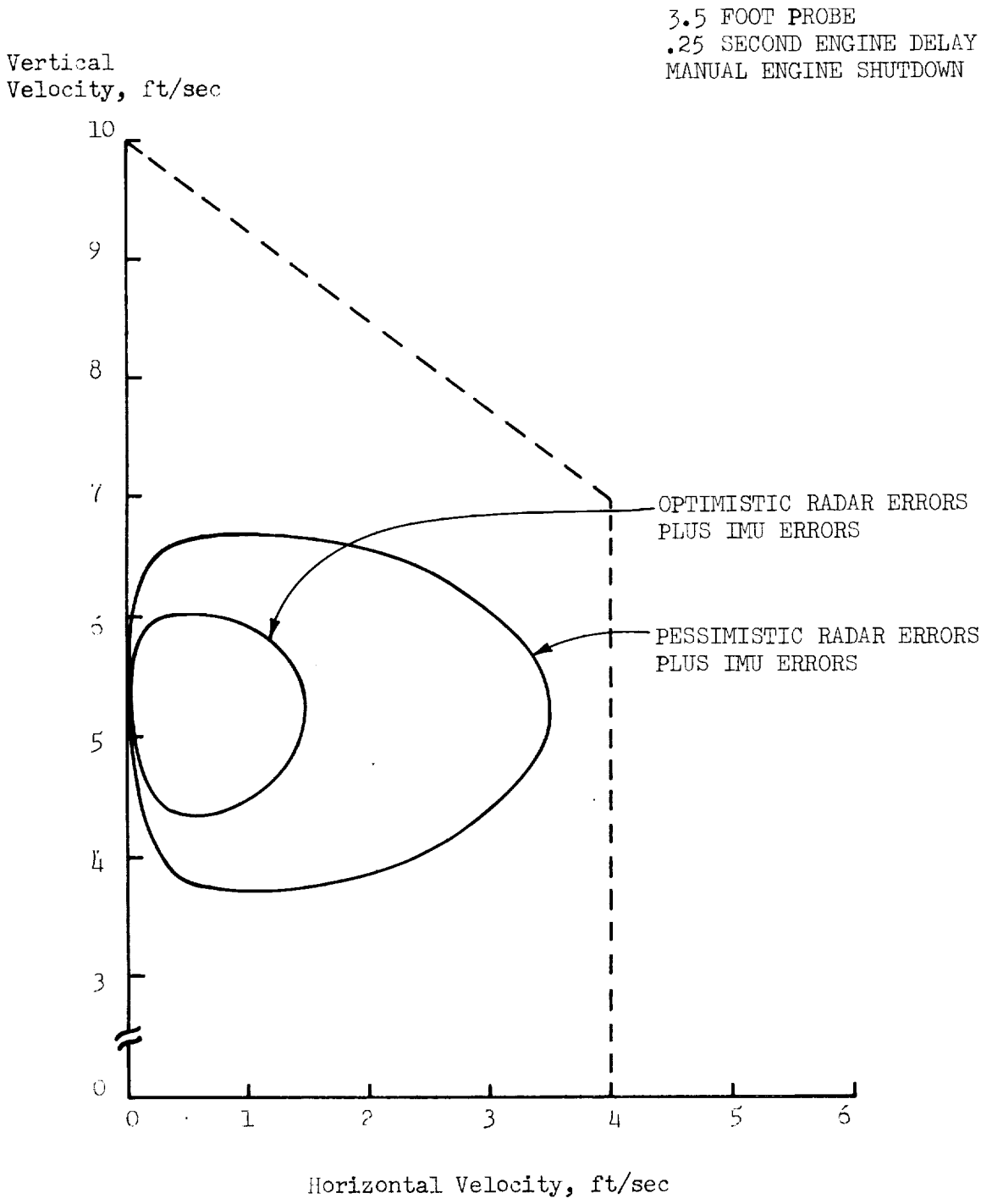

FIGURE 4. 0.99 PROBABILITY CONTOURS FOR TOUCHDOWN VELOCITY. (NO PILOT ERRORS)

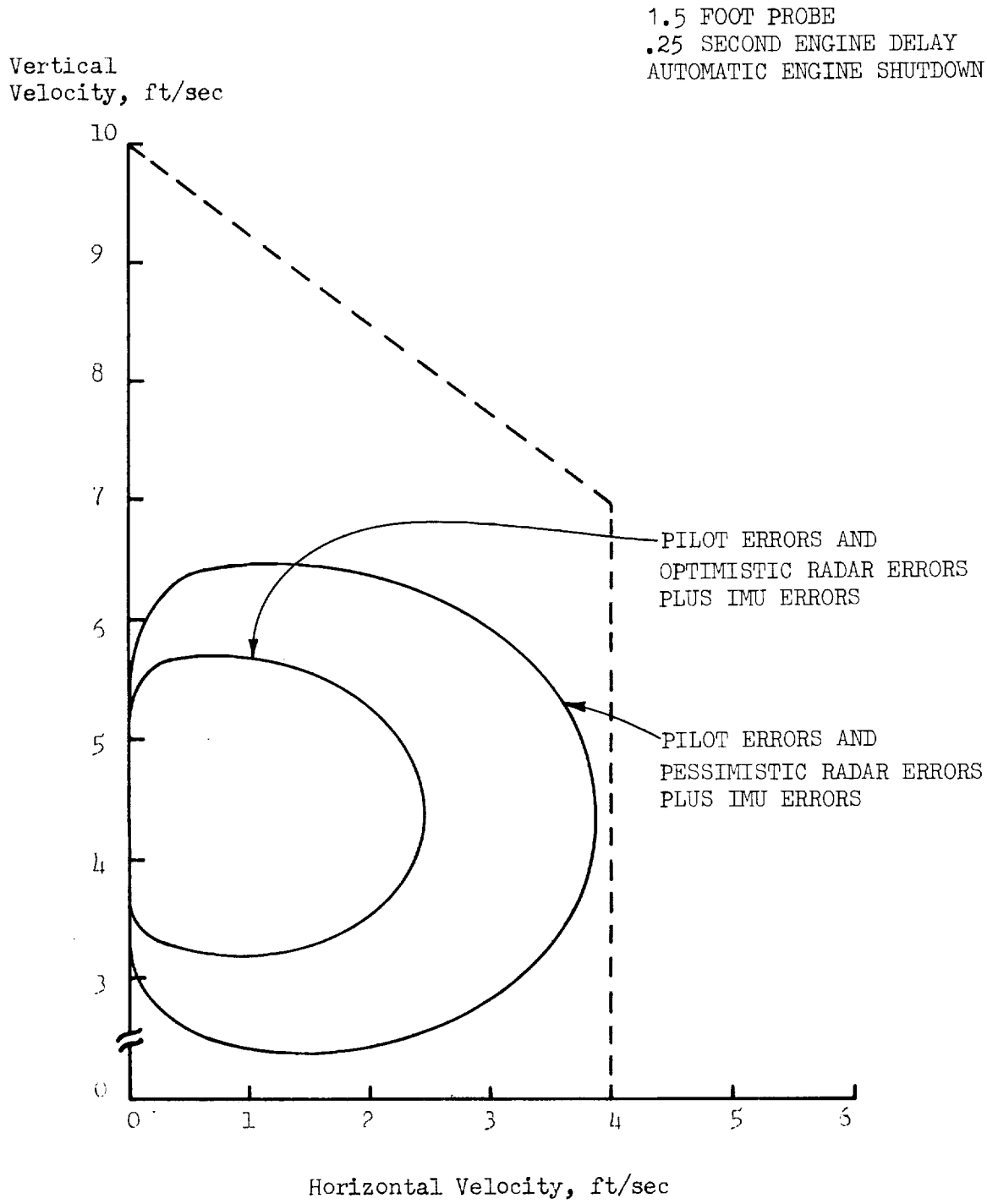

FIGURE 5. 0.99 PROBABILITY CONTOURS FOR AUTOMATIC ENGINE SHUTDOWN. (MODIFIED REFERENCE 1 DATA PLUS SYSTEM ERRORS)

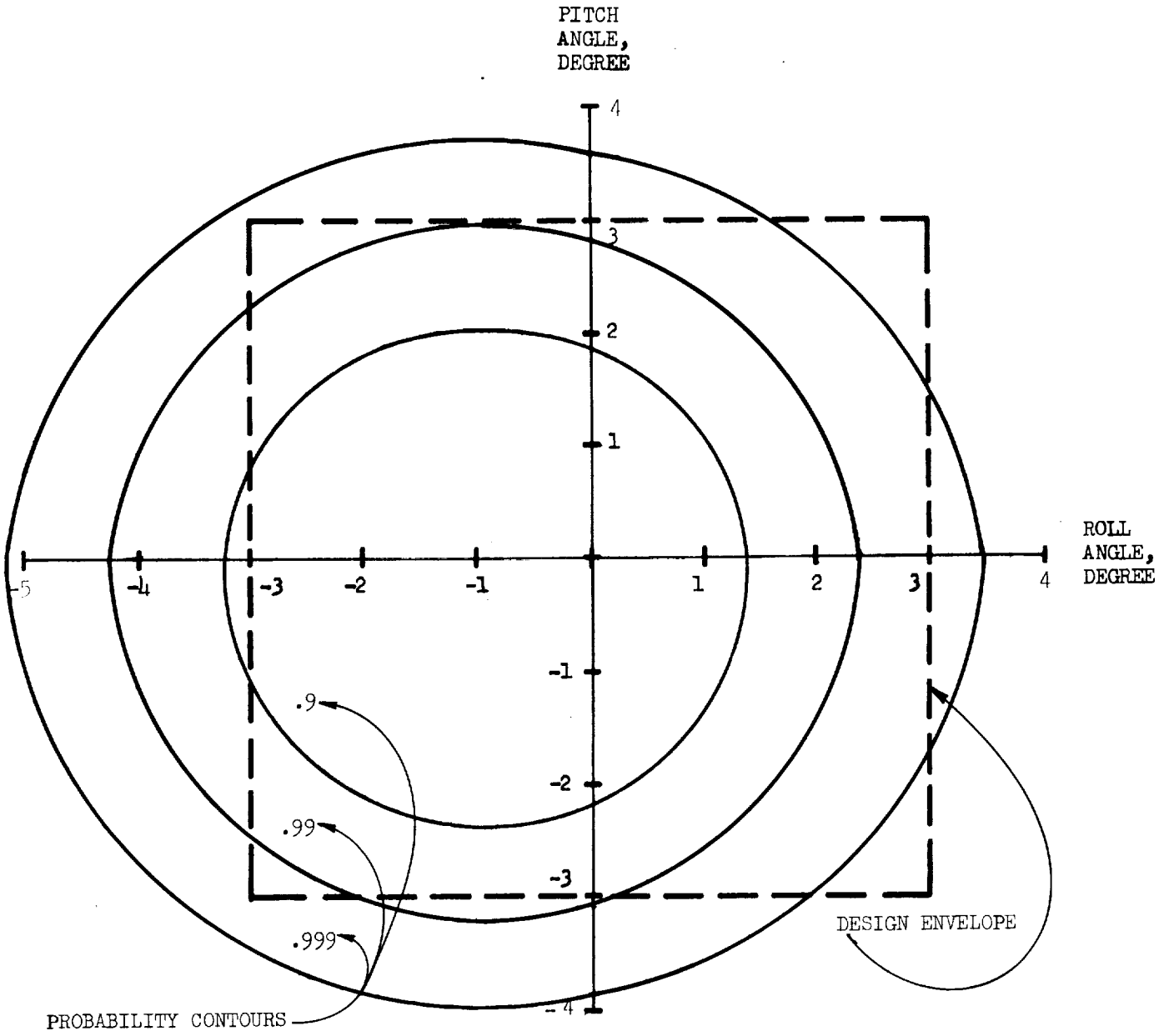

FIGURE 6. PROBABILITY CONTOURS FOR TOUCHDOWN ANGLES.
(NO C.G. UNCERTAINTY)

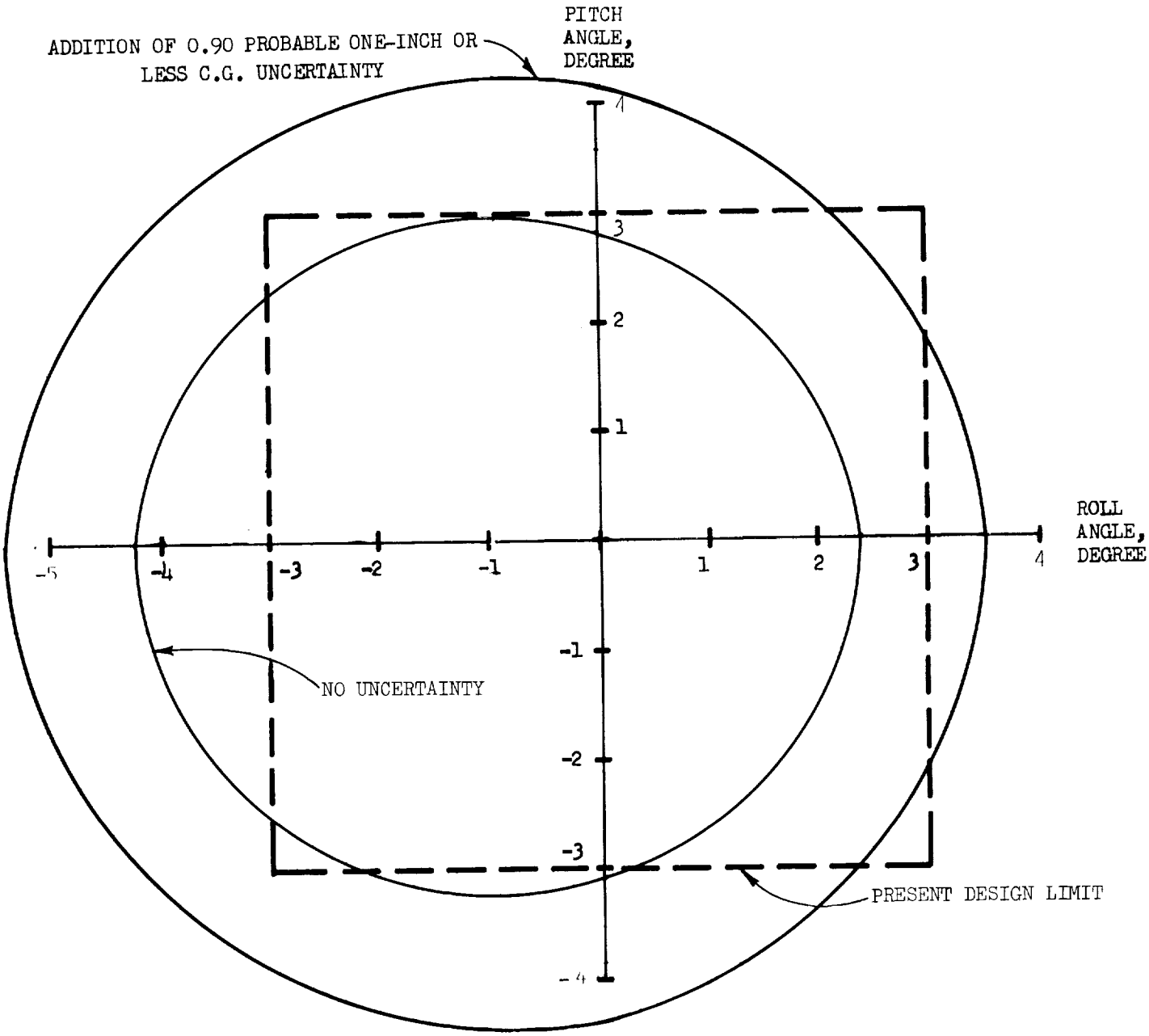

FIGURE 7. 0.99 PROBABILITY CURVES FOR TOUCHDOWN ANGLES IN PRESENCE OF 1 INCH 1σ C.G. UNCERTAINTY.

List of Symbols Used in Appendices

C_1, C_2	constants of integration
p	probe length
S	distance of vehicle drop after probe signal
t	time beginning from start of engine decay
V	horizontal velocity ($\sqrt{X^2 + Y^2}$)
X	forward velocity
Y	lateral velocity
Z	vertical velocity
Z_f	vertical velocity at touchdown
Z_p	vertical velocity at probe contact
δ	pilot reaction time plus system delay
Δt	time from t = 0 to touchdown
σ	standard deviation
μ	mean value

Appendix A

Equations for Determining Conditions at Probe Contact from Conditions at Touchdown

Assumptions:

1. Horizontal velocity, attitudes, and attitude rates remain constant between probe contact and touchdown.

2. Engine decay as e^{-25t}

3. T/W = 1 from probe light signal until start of engine thrust decay.

Basis for Assumptions:

1. Time between probe contact and touchdown is sufficiently small for assumption 1.

2. The time constant of the engine is .04.

3. The pilot was using ROD and the last input should be at 50 feet. This along with near zero attitudes should hold $T/W \simeq 1$.

With these assumptions;

$$\dot{Z} = g(1 - e^{-25t}) = 5.34\ (1 - e^{-25t})$$

$$Z = \int \dot{Z} dt = 5.34\left(t + \frac{1}{25} e^{-25t}\right) + C_1$$

Given at $t = 0$ $Z = Z_p$ from assumption 3

$$Z_p = \frac{5.34}{25} + C_1 \text{ or } C_1 = Z_p - \frac{5.34}{25}$$

Hence,

$$(1)\ Z = 5.34\left[t - \frac{1}{25}\left(1 - e^{-25t}\right)\right] + Z_p$$

Now,

$$S = \int Z dt = 5.34\left(\frac{t^2}{2} - \frac{t}{25} - \frac{1}{625}\right)e^{-25t} + Zpt + C_2$$

Given at $t = 0$ $S = Zp\delta$ from assumption 3

$$Zp\delta = \frac{-5.34}{625} + C_2 \text{ or } C_2 = Zp\delta + \frac{5.34}{625}$$

Therefore,

$$(2)\ S = 5.34\left[\frac{t^2}{2} - \frac{t}{25} - \frac{1}{625}\left(1 - e^{-25t}\right)\right] + Zp(t + \delta)$$

from (1) and when $t = \Delta t$ $Z = Z_f$

$$Z_f = 5.34\left[\Delta t - \frac{1}{25}\left(1 - e^{-25\Delta t}\right)\right] + Zp$$

From (2) and when $t = \Delta t$ $S = p$

$$p = 5.34\left[\frac{\Delta t^2}{2} - \frac{\Delta t}{25} - \frac{1}{625}\left(1 - e^{-25\Delta t}\right)\right] + Zp(\Delta t + \delta)$$

in (1) assume $\frac{5.34}{25} e^{-25\Delta t} \simeq 0$

in (2) assume $\frac{5.34}{625}\left(1 - e^{-25\Delta t}\right) \simeq 0$

from which

$$(3)\quad Z_f = 5.34\left(\Delta t - \frac{1}{25}\right) + Zp$$

$$(4)\quad p = 5.34\left(\frac{\Delta t^2}{2} - \frac{\Delta t}{25}\right) + Zp(\Delta t + \delta)$$

Solving for Δt in (3) gives

$$\Delta t = \frac{Zf - Zp}{5.34} + \frac{1}{25}$$

and

$$\Delta t^2 = \frac{Zf^2 - 2Z_fZ_p + Z_p^2}{5.34^2} + \frac{2(Z_f - Z_p)}{25(5.34)} + \cancel{\frac{1}{625}}^{\simeq 0}$$

from (4)

$$p = \Delta t^2 \frac{5.34}{2} - \Delta t \frac{5.34}{25} + Zp(\Delta t + \delta)$$

Substituting for Δt and simplifying gives

$$p = \frac{Z_f^2 - Z_p^2}{10.68} + Zp(\frac{1}{25} + \delta)$$

Solving for Zp,

$$Zp = 5.34(.04 + \delta) \pm \sqrt{28.52(.04 + \delta)^2 - 10.68 + Z_f^2}$$

This equation was used to determine vertical velocity at probe contact. Then further modifications to the data were made: (1) the engine delay time was changed from 0.15 to 0.25 second to reflect more realistic engine shutoff characteristics, (2) the probe length was changed from 3.0 to 3.5 feet, (3) the design descent rate schedule was changed from 4.0 to 3.5 feet/second (done by assuming that on each data run, the pilot would have reduced indicated rate of descent by 0.5 feet/second). After modifications of the data and selection of an error model, the data were then recalculated to give new touchdown conditions using the equation to solve from Zf,

$$Zf^2 = 10.68p + Zp^2 - 10.68\ Zp(.04 + \delta)$$

Appendix B

Calculation of Probability Contours for Velocities

Assumptions:

1. Z is normally distributed with mean μ_2 and variance σ_2^2
2. X, Y are normally distributed with mean 0 and variance σ_1^2.
3. X, Y, and Z are mutually independent.

Basis for Assumptions:

1. Sample means and standard deviations of X, Y, and Z were computed. They were:

$$\bar{X} = -.0867; \quad \sqrt{\frac{\Sigma(X_i - \bar{X})^2}{299}} = 1.0577$$

$$\bar{Y} = .0301; \quad \sqrt{\frac{\Sigma(Y_i - \bar{Y})^2}{299}} = 1.1104$$

$$\bar{Z} = 5.6289; \quad \sqrt{\frac{\Sigma(Z_i - \bar{Z})^2}{299}} = .6443$$

2. The χ^2 contingency table test accepted the hypotheses that X, Y, and Z were mutually independent.

3. The Kolmogorov-Smirnov test accepted the hypotheses that X, Y, and Z were normally distributed with the above means and standard deviations.

4. The F test accepted the hypothesis that X and Y had equal variances.

5. The t-test accepted the hypothesis that X and Y had mean 0.

6. Based on the assumptions that X and Y had means of 0 and the same variance σ_1^2, a new estimate of σ_1^2 was calculated.

$$\sigma_1^2 = \frac{\Sigma X_i^2 + \Sigma Y_i^2}{600} = (1.0845)^2$$

7. As a final check, the Kolmogorov-Smirnov test was used to test the hypotheses that X and Y were distributed $N(0,(1.0845)^2)$. These hypotheses were acceptable.

Calculation of Probabilities Within Contours

Let $V = \sqrt{X^2 + Y^2}$. Under the assumptions given, V is distributed as $\sigma_1\sqrt{\chi^2(2)}$ where $\chi^2(2)$ represents a central chi-square random variable with 2 degrees of freedom. The cumulative distribution function of V, $F_V(v)$, is given by

$$\Pr\left\{V \leq v\right\} = \Pr\left\{V^2 \leq v^2\right\} = \Pr\left\{\sigma_1^2 \chi^2(2) \leq v^2\right\} = \Pr\left\{\chi^2(2) \leq \frac{v^2}{\sigma_1^2}\right\}$$

$$= \int_0^{\frac{v^2}{\sigma_1^2}} \frac{1}{2} e^{-\frac{x}{2}} dx = 1 - e^{-\frac{v^2}{2\sigma_1^2}}$$

The probability density function of V is given by

$$f_V(v) = \frac{dF_V(v)}{dv} = \frac{v e^{-\frac{v^2}{2\sigma_1^2}}}{\sigma_1^2} \qquad (1)$$

Because Z is assumed normally distributed with mean μ_2 and variance σ_2, the probability density function of Z is

$$f_Z(Z) = \frac{1}{\sigma_2\sqrt{2\pi}} e^{-\frac{(Z-\mu_2)^2}{2\sigma_2^2}} \qquad (2)$$

Because V and Z are independent, the joint p.d.f. is the product of the two p.d.f.'s. The probability that a sample value of Z and V, (V_0, Z_0) will lie within a given area A in the V, Z plane (see illustration

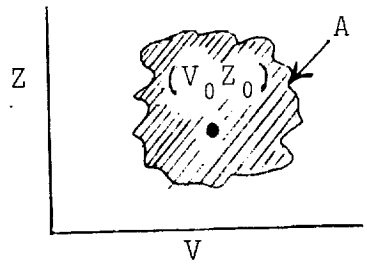

is given by

$$\int_A f_V(v) f_Z(Z) dA \qquad (3)$$

A probability contour is the locus of all points (V, Z) such that $f_V(V)f_Z(Z)$ is a constant p. Thus, the point (V_o, Z_o) falls on the contour of height p if

$$f_V(V_o)f_Z(Z_o) = p; \text{ i.e., if}$$

$$\frac{1}{\sigma_1^2 \sigma_2 \sqrt{2\pi}} e^{-\frac{(Z_o-\mu_2)^2}{2\sigma_2^2}} V_o e^{-\frac{V_o^2}{2\sigma_1^2}} = p; \text{ i.e., if}$$

$$p = KV_o e^{-\left[\frac{(Z-\mu_2)^2}{2\sigma_2^2} + \frac{V_o^2}{2\sigma_1^2}\right]} \qquad \text{where } K = \frac{1}{\sigma_2 \sqrt{2\pi}\, \sigma_1^2}$$

or, taking logarithms,

$$\log\left(\frac{K}{P}\right) = \frac{(Z_o - \mu_2)^2}{2\sigma_2^2} + \frac{V_o^2}{2\sigma_1^2} - \log V_o. \tag{4}$$

The area, A(p), defined by (4) is shown below

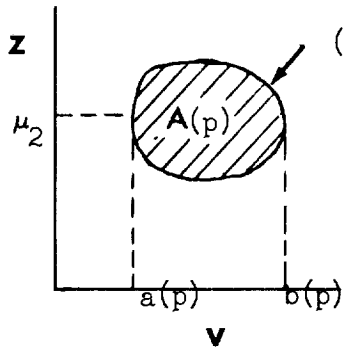

$$(Z-\mu_2)^2 = 2\sigma_2^2\left[\log\left(\frac{K}{P}\right) - \frac{V^2}{2\sigma_1^2} + \log V\right]$$

The points a(p) and b(p) are such that when V takes on those values in equation (4), Z is equal to μ_2. Because f_Z is symmetric about μ_2, the probability given by (3) can be calculated by integrating over the upper half of the area in figure 2 and multiplying the result by 2.

Thus (3) becomes

$$\Pr\left\{(V_c, Z_o) \epsilon A(p)\right\} \sigma_1^2 \sigma_2 \sqrt{2\pi} \int_{a(p)}^{b(p)} V e^{-\frac{V}{2\sigma_1^2}} \int_{\mu_2}^{g(V)} e^{-\frac{(Z-\mu_2)^2}{2\sigma_2^2}} dz\, dV \qquad (5)$$

where $g(V) = \sqrt{2\sigma_2^2 \left[\log\left(\frac{k}{p}\right) - \frac{V^2}{2\sigma_1^2} + \log V\right]}$

Values of (5) for various values of p are given below:

p	$\Pr\left\{(V_o, Z_o) \epsilon A(p)\right\}$
.0394	.900
.0202	.950
.0103	.975
.0042	.990
.0039	.999

Calculation of Probability Contours for Roll and Pitch Angles

The data on the roll and pitch angles, Θ and ϕ, did not belie the assumption of independence and normality. On this assumption, if Θ is normally distributed with mean μ_Θ and variance σ_Θ^2 and ϕ is normally distrubuted with mean μ_ϕ and variance σ_ϕ^2, then, the probability contours for Θ and ϕ are ellipses of the form

$$\frac{(\Theta - \mu_\Theta)^2}{2\sigma_\Theta^2} + \frac{(\phi - \mu_\phi)^2}{2\sigma_\phi^2} = c^2$$

where $1 - e^{-c^2}$ is the probability of falling inside the ellipse.

Reference - H. Cramér - Mathematical Methods of Statistics, Princeton University Press, 1946, p.288.

Appendix C

Calculation of Probability of Landing in Design Envelope

Suppose it is wished to calculate the probability of landing within the envelope shown below. Using the method discussed in Appendix B,

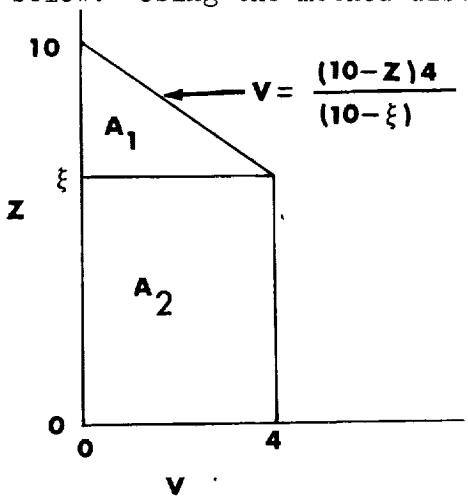

The area A referred to in that appendix is now equal to $A_1 + A_2$ as shown above.

Thus $$\int_A f(Z)f(V)\,dA = \int_{A_1} f(Z)f(V)\,dA + \int_{A_2} f(Z)f(V)\,dA$$

Note that

$$\int_{A_1} f(Z)f(V)\,dA_1 = \int_{\xi}^{10} f(Z)\left[\int_{o}^{\frac{4(10-Z)}{(10-\xi)}} f(V)dV\right] dZ$$

$$= \int_{\xi}^{10} f(Z)\, F_V\left[\frac{40-4Z}{10-\xi}\right] dZ$$

$$= \int_{\xi}^{10} \left[1 - e^{-\frac{\left(\frac{40-4Z}{10-\xi}\right)^2}{2\sigma_1^2}}\right] \frac{1}{\sigma_2\sqrt{2\pi}} e^{\frac{-(Z-\mu_2)^2}{2\sigma_2^2}} dZ$$

$$= \int_{\xi}^{10} \frac{1}{\sigma_2\sqrt{2\pi}} e^{\frac{-(Z-\mu_2)^2}{2\sigma_2^2}} dZ - \frac{1}{\sigma_2\sqrt{2\pi}} \int_{\xi}^{10} e^{-\frac{\left(\frac{40-4Z}{10-\xi}\right)^2}{2\sigma_1^2}} e^{\frac{-(Z-\mu_2)^2}{2\sigma_2^2}} dZ$$

$$= \Phi\left(\frac{10 - \mu_2}{\sigma_2}\right) - \Phi\left(\frac{\xi - \mu_2}{\sigma_2}\right) - Q$$

where $Q = \frac{1}{\sigma_2\sqrt{2\pi}} \int_{\xi}^{10} e^{\frac{-M(Z-10)^2}{2\sigma_1^2}} \; e^{\frac{-(Z-\mu_2)^2}{2\sigma_2^2}} \; dZ$

$$\text{and } M = \frac{16}{(10-\xi)^2}$$

Let E equal the absolute value of the exponent in the integrand of Q.

$$\text{Then } E = \frac{M(Z-10)^2}{2\sigma_1^2} + \frac{(Z-\mu_2)^2}{2\sigma_2^2}$$

$$= \frac{\sigma_1^2(Z-\mu_2)^2 + M\sigma_2^2(Z-10)^2}{2\sigma_1^2\sigma_2^2}$$

$$= \frac{(\sigma_1^2 + M\sigma_2^2)Z^2 - 2(\mu_2\sigma_1^2 + 10M\sigma_2^2)Z + \sigma_1^2\mu_2^2 + 100M\sigma_2^2}{2\sigma_1^2\sigma_2^2}$$

$$= \frac{Z^2 - 2\left[\frac{\mu_2\sigma_1^2 + 10M\sigma_2^2}{\sigma_1^2 + M\sigma_2^2}\right] Z + \left[\frac{\sigma_1^2\mu_2^2 + 100M\sigma_2^2}{\sigma_1^2 + M\sigma_2^2}\right]}{2\,\frac{\sigma_1^2\sigma_2^2}{\sigma_1^2 + M\sigma_2^2}}$$

Let $\Gamma = \frac{\sigma_1^2\mu_2^2 + 100M\sigma_2^2}{\sigma_1^2 + M\sigma_2^2}$

$$\text{Then } E = \frac{Z^2 - 2\left[\frac{\mu_2\sigma_1^2 + 10M\sigma_2^2}{\sigma_1^2 + M\sigma_2^2}\right] Z + K^2 + (\Gamma - K^2)}{2\left[\frac{\sigma_1^2\sigma_2^2}{\sigma_1^2 + M\sigma_2^2}\right]} \quad \text{for any K.}$$

Let $K = \left[\frac{\mu_2\sigma_1^2 + 10M\sigma_2^2}{\sigma_1^2 + M\sigma_2^2}\right]$ and $D^2 = \frac{\sigma_1^2\sigma_2^2}{\sigma_1^2 + M\sigma_2^2}$

Then $E = \frac{(Z^2 - 2KZ + K^2) + (\Gamma - K^2)}{2D^2} = \frac{(Z - K)^2 + \Gamma - K^2}{2D^2}$

Thus, $Q = \frac{1}{\sigma_2\sqrt{2\pi}} \int_{\xi}^{10} e^{-E}\, dZ = \frac{1}{\sigma_2\sqrt{2\pi}} \int_{\xi}^{10} e^{-\frac{(Z-K)^2}{2D^2}} e^{-\frac{(\Gamma-K^2)}{2D^2}}\, dZ$

Let $S = \frac{De^{\frac{K^2-\Gamma}{2D^2}}}{\sigma_2}$. Then $Q = \frac{S}{D\sqrt{2\pi}} \int_{\xi}^{10} e^{-\frac{(Z-K)^2}{2D^2}}\, dZ$

$$= S\left[\Phi\left(\frac{10-K}{D}\right) - \Phi\left(\frac{\xi-K}{D}\right)\right]$$

Therefore, using equations (2) and (3), it follows that

$$\int_{A_1} f(Z)f(V)dA_1 = \Phi\left(\frac{10-\mu_2}{\sigma_2}\right) - \Phi\left(\frac{\xi-\mu_2}{\sigma_2}\right) - S\,\Phi\left(\frac{10-K}{D}\right) + S\,\Phi\left(\frac{\xi-K}{D}\right)$$

Now,

$$\int_{A_2} f(Z)f(V)dA_2 = \Pr\{Z \leq \xi\} \quad \Pr\{V \leq 4\}$$

$$= \left(\Phi\left[\frac{\xi-\mu_2}{\sigma_2}\right]\right)\left(\left[1 - e^{\frac{-(4)^2}{2\sigma_1^2}}\right]\right)$$

Thus, $\Pr\{\text{landing in the shown envelope}\}$ is equal to

$$\Phi\left(\frac{10-\mu_2}{\sigma_2}\right) - \Phi\left(\frac{\xi-\mu_2}{\sigma_2}\right) e^{-\frac{8}{\sigma_1^2}} - S\,\Phi\left(\frac{10-K}{D}\right) + S\,\Phi\left(\frac{\xi-K}{D}\right)$$

where $D = \dfrac{\sigma_1\sigma_2}{\sqrt{\sigma_1^2 + M\sigma_2^2}}$

$$S = De^{\frac{\Gamma-K^2}{2D^2}}$$

$$\Gamma = \frac{\sigma_1^2\mu_2 + 100M\sigma_2^2}{\sigma_1^2 + M\sigma_2^2}\,, \quad K = \frac{\mu_2\sigma_1^2 + 10M\sigma_2^2}{\sigma_1^2 + M\sigma_2^2}$$

and $M = \dfrac{16}{(10-\xi)^2}$